Astron. Astrophys. 313, 649–656 (1996)

ASTRONOMY AND ASTROPHYSICS

Diffuse interstellar bands: resolved rotational band structure at 5850 Å*

P. Jenniskens[1], I. Porceddu[2], P. Benvenuti[3], and F.-X. Désert[4]

[1] NASA/Ames Research Center, Mail Stop 239-4, Moffett Field, CA 94035-1000, USA
[2] Stazione Astronomica, Via Ospedale 72, I-09124 Cagliari, Italy
[3] Space Telescope - European Coordinating Facility, European Southern Observatory, Karl-Schwarzschild-Strasse 2, D-85748 Garching bei München, Germany
[4] Institut d'Astrophysique Spatiale, Bat 121, Université Paris XI, F-91405 Orsay Cedex France

Received 23 October 1995 / Accepted 14 February 1996

Abstract. The only candidate of what may be a resolved rotational vibrational band in the DIB Survey of Jenniskens & Désert (1994), the triplet of bands at 5844, 5850 and 5852 Å, is examined in detail in order to establish the nature of these DIBs. We find that superposed on the broad λ5844 are four weak features, reminiscent of substructure found on top of the broad λ5778. The relative band strength of DIBs λ5844 and λ5850 correlates with the rotational temperature in the J = 0 and J = 1 levels of molecular hydrogen. However, we do not find variations in band shape that are consistent with substructure of a resolved rotational band profile. Instead, the narrow λ5850 is found to have a shoulder on the red and blue side of the main band, which can imply that this band itself is an unresolved rovib band with P, Q and R branches.

Key words: interstellar medium: molecules – molecular processes

1. Introduction

Some of the "diffuseness" of Diffuse Interstellar Bands (DIB) in the spectra of reddened stars may be due to unresolved rotational-vibrational (rovib) band structure (e.g. Danks & Lambert 1976, Douglas 1977, Cossart-Magos & Leach 1990). Such rotational broadening can be recognized by multiple peaks, shoulders or wings caused by the progressions of rotational lines called the P, Q and R branches that result from the optical selection rules ΔJ = -1, 0, +1 respectively. The presence of rotational structure in DIBs has not been established beyond doubt, although several authors have interpreted some shoulders and red gradings as such (Welter & Savage 1977, Hayden-Smith et al. 1981, Snell & Vanden Bout 1981, Herbig & Soderblom 1982). The Doppler broadening from turbulent motion in the interstellar medium blends potential rovib structure into a featureless profile in most lines of sight. However, recent high spectral resolution studies of band profiles in lines of sight with small turbulent velocity dispersion have shown promising peaks on the main band of DIB λ6613 (Hibbins, Miles & Sarre 1995 - see also the recent paper by Sarre et al. 1995). Of course, these subpeaks can also be a mere coincidental superposition of DIBs, which is not unlikely given the high density of DIBs in this spectral region. Further evidence of rovib structure is called for.

We made an attempt to find rovib profiles broad enough to be resolved in the DIB Survey of Jenniskens & Désert (1994). Such profiles could come from a carrier with at least one low moment of inertia so that the intrinsic band is much wider than the interstellar turbulent broadening. Indeed, several pairs of DIBs qualify as a possible rovib profile with no Q-branch (when optical selection rules inhibit ΔJ = 0). However, such profiles are easily confused with two DIBs that nearly coincide in position. On the other hand, and this is a very significant point we believe, there is only one case of what may be a resolved rovib profile with a central Q-branch: the broad λ5844 in combination with the narrow λ5850 and a possible broad band at 5852 Å (Fig. 1). That case deserves some further attention and is the topic of this paper.

The bands at 5844 and 5850 Å were recognized by Herbig (1975) and most recently studied by Krelowski et al. (1993). In this paper, we examine the profile shapes of these DIBs and search for changes in band shape as a function of local kinetic gas temperature.

2. Observations

Very high signal to noise observations of the wavelength range 5830-5860 Å were obtained at the Observatoire d'Haute

Send offprint requests to: P. Jenniskens (peter@max.arc.nasa.gov)

* From observations at OHP and ESO.

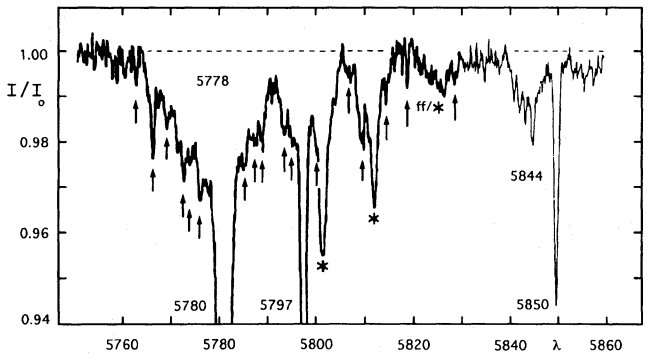

Fig. 1. The location of λ5850 and λ5844 relative to the well known DIBs at 5780 and 5797 Å. This is in an average of five high signal-to-noise spectra from OHP with a spectral resolution of 0.3 Å. The position of known weak diffuse interstellar bands (Jenniskens & Désert 1993) are marked by arrows. Throughout this paper, stellar lines are marked with an asterisk. This spectrum is a weighted mean of five background stars: HD216532 (O8V, E_{B-V} = 0.86), HD216898 (O9V, 0.85), HD15558 (O5III, 0.83), BD+31 643 (B5V, 0.85), and HD239729 (O9V, 0.66).

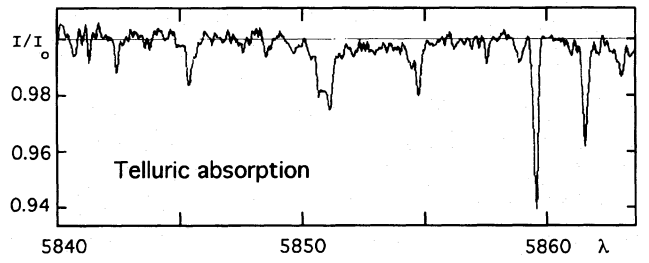

Fig. 2. Atmospheric lines in the high resolution spectrum of standard star HD120315 (B3V, E_{B-V} = 0.011, Vsin(i) = 205 km/s) at zenith distance of 70 degrees. OHP data from Sept. 27, 1991.

Provence (OHP) in France and at the European Southern Observatory (ESO) in Chile.

Observations collected at ESO were obtained at the 1.4m CAT Telescope, by using the CES configured with the Short Camera and the 1024 x 640 pixels RCA SID 503 CCD detector. The resolving power was set to R ∼ 60,000, with an effective resolution of about 0.098 Å. Spectra were obtained in August of 1992. Observations collected at OHP were obtained with the 1.5m Coude Telescope, using the Aurelie spectrograph in low (0.3 Å) or high (0.098 Å) resolution mode (Gillet 1990, Jenniskens & Désert 1993). Spectra were obtained in 1990 and 1991 as part of a different program (Désert et al. 1995) and some others in 1992.

All spectra were corrected for CCD pixel-to-pixel sensitivity variations by flatfielding, after subtracting the contribution from dark current. Cosmic ray hits were removed by interpolation of adjacent pixels. Telluric lines were removed by scaling the lines to those in the spectrum of a fast rotating B3V standard star, which is relatively devoid of stellar lines. A linear baseline was applied, unless specified, in order to reveal any broad shallow DIBs.

Table 1. Stellar lines identified in standard star spectra from multiplet tables by Moore (1945). Symbols of line strength: s = strong, m = medium, w = weak, v = very. Standard stars: HD47839 (O7Vf), HD36879 (O7III), HD214680 (09V), HD37367 (B2V), HD23060 (B3V), HD205021 (B1 III), HD35468 (B2 III), HD206165 (B2Ib), HD169454 (B1Ia), and HD34085 (B8Ia).

λ(Å) ±0.3 Å	ident.	λ_r	O	BV	B1III	B0-2I	B7-8I
5826.3	-		s	-	-	-	-
5827.4	SiII 8	5827.80	-	-	-	-	m
	CII 8	5827.80					
5829.3	NI 32	5829.53	-	-	vw	-	vw
5834.0	-		w	m	s	s	m
5836.5	CII 22	5836.31	-	-	-	-	vw
5842.0	-		-	-	vw	-	-
5843.7	CII 22	5843.77	-	-	vw	-	-
5846.0	SiII 8	5846.12	-	-	-	-	m
5849.2	-		-	-	m	-	-
5852.5	Ne I 6	5852.49	-	-	-	w	m
5853.5	NI 32	5854.16	-	-	-	vw	vw
5856.0	CII 22	5856.09	-	-	m	w	w
5860.0	-		-	vw	w	-	w
5864.2	-		-	vw	vw	-	-
5867.5	SiII 8	5867.50	vw	-	vw	-	m
5868.2	SiII 8	5868.40	vw	-	w	-	m
5876.0	HeI 11	5875.65	vs	vs	vs	vs	vs

In order to access the presence of possible new DIBs or weak features on DIB profiles, it is important to exclude the possibility that the absorptions are photospheric, telluric or instrumental in origin.

The telluric absorptions in the spectral range of interest are mostly due to water in the Earth's atmosphere (Fig. 2). They are easily recognized and can be efficiently removed.

Photospheric absorptions arise in the atmosphere of the program star. Some emission lines originate in the HII region or reflection nebula that surrounds some of the typical early type program stars. These lines are not removed from the spectra. They are identified from the spectra of unreddened (or weakly reddened) standard stars (Table 1) and marked by an asterisk in the figures.

Instrumental features result from non-perfect flatfielding of the CCDs, imperfect deglitching, and cosmic rays. Flatfield remnants can cause spurious absorptions in high signal-to-noise data, which are not fully removed by averaging many spectra. For that reason, it is prudent to compare high signal-to-noise spectra to those obtained with different CCD detectors at other observatories.

3. Results

3.1. The general shape of the bands

The topic of study in this paper is the spectral region between 5830 and 5860 Å, the right part of Fig. 1, where a narrow λ5850

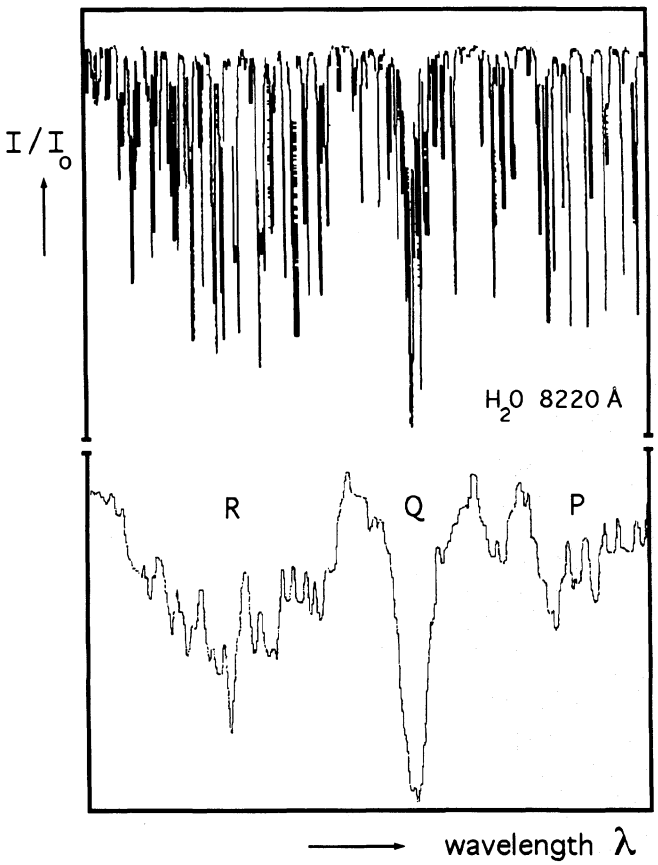

Fig. 3. Rovib profile of the 8220 Å band of water before and after smoothing with a 10-pixel (3 Å) box function.

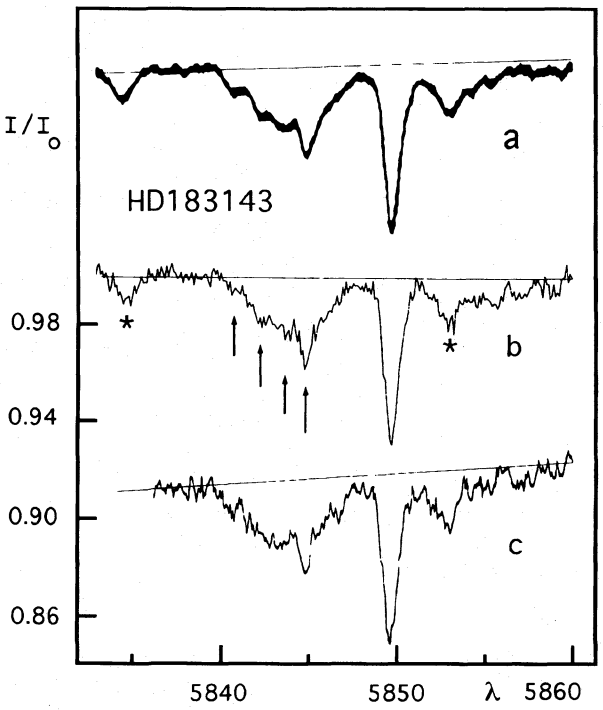

Fig. 4a–c. HD183143 (B7Ia, E_{B-V} = 1.24, Vsin(i) = 60 km/s) - at a resolution of 0.1 Å from spectra obtained at CFHT (**a** Herbig 1993), OHP (**b** this work), and CFHT (**c** Krelowski et al. 1993).

is flanked by a broad λ5844 and perhaps a broad λ5852. Compare the shape of these bands to a classical example of a resolved rovib band shown in Fig. 3. This is the 8220 Å band of water, observed at OHP by the same instrument and smoothed by a 10 pixel (3 Å) box smoothing function to mimic the effect of Doppler broadening. Note the similarity in the shape of this smoothed rovib band and the 5844/5850 DIBs. Although this shows that some resolved rovib profiles can exist that are similar in shape to this pair of DIBs, whether or not these DIBs together form a rovib profile will now be examined.

3.2. Does λ5844 show substructure?

First of all, we find that the DIB spectrum at 5850 Å is rich in weak DIBs. Fig. 1 shows four intriguing features superposed on the broad λ5844. Previously, we reported on similar weak DIBs superposed on nearby broad λ5778 (Jenniskens & Désert 1993) and argued that some of these features may well be substructure, given that similar structure is present in another DIB at 6284 Å. We will now examine whether the features superposed on λ5844 are DIBs and, if so, whether they are part of the underlying band.

We will start the discussion with the spectrum of HD183143. This is a late B7Ia super giant star and of different spectral type than the O-type stars gathered in Fig. 1. HD183143 was observed at high resolution at OHP and the result is shown in Fig. 4. We recognize the same four features on λ5844, although the relative band strength varies and the broad DIB itself is relatively stronger. The features are also broader due to the large spread in radial velocities of cloud components in the line of sight. The spectrum compares well to similar data by Herbig (1993) and Krelowski et al. (1993), both obtained at the Canada-France-Hawaii Telescope (CFHT). The four features in Fig. 1 are present in all spectra and therefore not instrumental of origin, that is due to imperfect corrections for pixel-to-pixel sensitivity variations of the CCD. Detailed comparison shows some small variations in wavelength scale, and in the choice of the baseline. There are also minor differences between Herbig's spectrum and the OHP spectrum at wavelengths above 5850 Å. Other differences can be ascribed to noise. Note that the spectra of Krelowski et al. are not corrected for telluric absorption, but the telluric lines are so weak that they can not be recognized.

Similar high resolution spectra of early B-type super giants are shown in Fig. 5. These spectra were obtained by us at ESO. The four weak features are present again. At this resolution, the effect of Doppler motion in the clouds is clearly seen. Notably λ5850 and the weak λ5845 are broadened in HD152234 as compared to HD152236.

Finally, we note that these features are also present in several spectra of other reddened stars published in the literature (Josafatsson & Snow 1987, Herbig 1993, Krelowski et al. 1993). Fig. 6, for example, reproduces the four spectra of highest signal-to-noise published by Krelowski et al. in the Astrophysical Journal. The features are also present in the o-Per spectra of Krelowski & Sneden (1993) and they do not shift with the

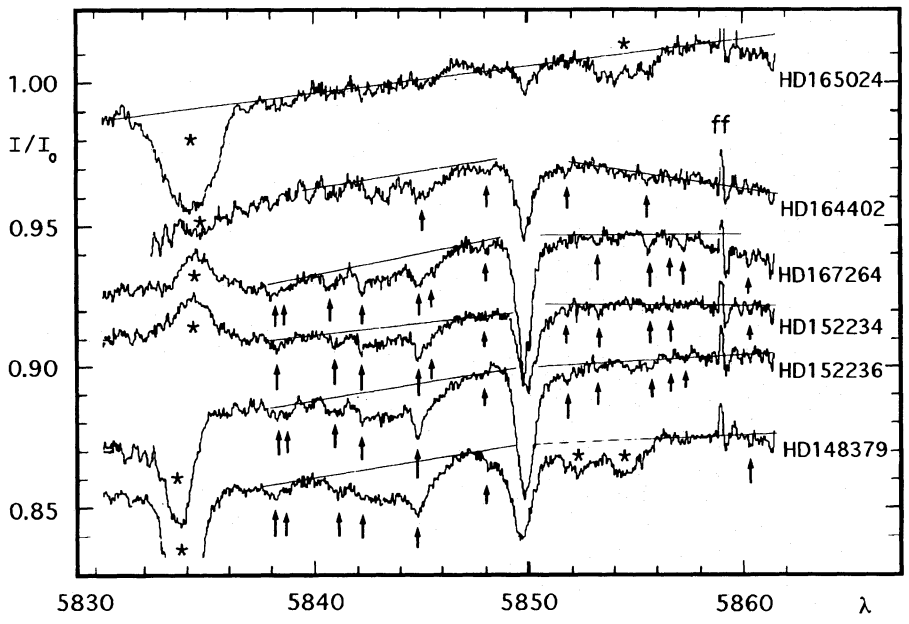

Fig. 5. High resolution (0.1 Å) spectra taken at ESO. No baseline was subtracted from these data. Arrows mark possible DIBs. From top to bottom (Vsin(i) from Bernacca & Perinotto 1970): HD165024 (B2Ib, E_{B-V} = 0.13, Vsin(i) = 95 km/s), HD164402 (B0Iab, 0.20, 90 km/s), HD167264 (B0.5Ia, 0.28, 85 km/s), HD152234 (B0.5Ia, 0.41, 85 km/s), HD152236 (B1Iae, 0.69, 60 km/s), and HD148379 (B2Ia, 0.74, 60 km/s). The spectra are displaced by 0.00, -0.03, -0.07,-0.08,-0.10, and -0.13 respectively in units of normalised intensity I/I_o.

line of sight position of the double star pair, consistent with an origin of the features in the interstellar medium and excluding an origin in the photosphere of the star.

3.3. Other weak DIBs

Many other weak and narrow features are recognized in the CES spectra of Fig. 5, notably in the lines of sight that have a relatively weak band λ5844. Note that these stars are fast rotators in all cases with stellar lines much wider than the weak features, which excludes a photospheric origin. A telluric origin is also excluded. A remnant due to instrument flatfielding is present in the data (marked ff). While the flatfielding remnant is of similar strength in all spectra, the proposed DIBs are seen in some of the spectra but not in all. The evidence for their existence is less strong than for the four strongest features. However, some further support comes from a high resolution spectrum of HD30614 obtained at OHP with a different CCD detector (Fig. 7), which shows the same weak absorption features.

All weak DIBs are listed in Table 2. The Full Width at Half Maximum (FWHM) and the depth of the lines were measured, from which W/E_{B-V} (in mÅ per magnitude) is calculated assuming a Gaussian shape for the profiles: W = 1.0645 × Ac × FWHM. Error estimates are not given, because the equivalent width is affected by unknown errors related to their relative low strength and the difficulty of placing the baseline.

This list includes a feature at λ5846.0, which is not seen as a peak in the spectra itself, but needs to be included when a sum of Gaussian profiles is used to fit the profile in order to account for the relatively sharp decrease of absorptivity in the long wavelength wing of λ5844. It is at present not clear if this feature is an independent DIB or just part of a non-gaussian λ5844 itself.

3.4. A P branch at 5852 Å?

How about a possible weak DIB longward of λ5850 that could be the P branch of a rovib profile? Indeed, some spectra suggest the presence of a weak shallow DIB longward of λ5850. Fig. 4, for example, shows that the spectrum of HD183143 stays below the chosen baseline between 5851 and 5858 Å for given baseline. A similar depression is seen in the spectra of HD148379 (B2Ia - Fig. 5) and HD210839 (O6If - Fig. 6), but not in other spectra. We note that these stars are also the ones with a strong broad λ5844. Broad DIBs usually respond in a similar manner to environmental changes (Jenniskens & Désert 1995), which argues in favor of a broad DIB at this position. The depth of this band is about 0.5 times the depth of λ5844 and its central position is at about 5852 Å.

The true nature of this depression remains in doubt, however. The measured depth is sensitive to the choice of the baseline. Also, there are stellar lines at 5852.5 (medium strong), 5853.5 (weak) and 5856.0 (weak) in B-type super giants, but these seem to be responsible for only part of the absorption, except perhaps in HD148379. In addition, there are some narrow DIBs, one of which is at 5853.2 Å (Fig. 5), which contribute to the total absorption. Again, these may not account for all absorption in this region. At present, the evidence for such shallow broad DIB is not sufficient to mark it as either "certain" (+) or even "probable" (o).

3.5. The shape of 5850

Finally, let us examine the band profiles of λ5850 in those lines of sight with smallest Doppler broadening (Fig. 8). We find that λ5850 has a narrow central peak and two shoulders, one on the blue and one on the red side. In addition, there is sometimes a fairly broad band underlying the red foot of the DIB, with strong intensity variations from one profile to the other. We surmise

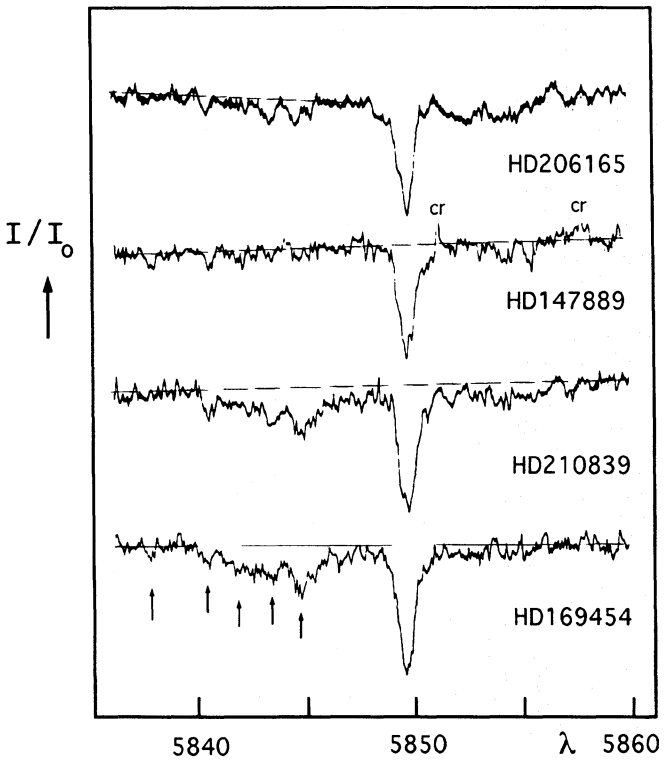

Fig. 6. The spectra of highest signal-to-noise from Krelowski et al. (1993). The published results (CFHT data) were scanned from the publication in Astrophysical Journal, reordered, enlarged, and subsequently scaled to approximately equal λ5850 strength. The spectra are not corrected for telluric absorption. From top to bottom: HD206165 (B2Ib, E_{B-V} = 0.46, Vsin(i) = 15 km/s), HD147889 (B2V, 1.07, 100), HD210839 (O6If, 0.55, -), and HD 169454 (B1Ia, 1.13, -).

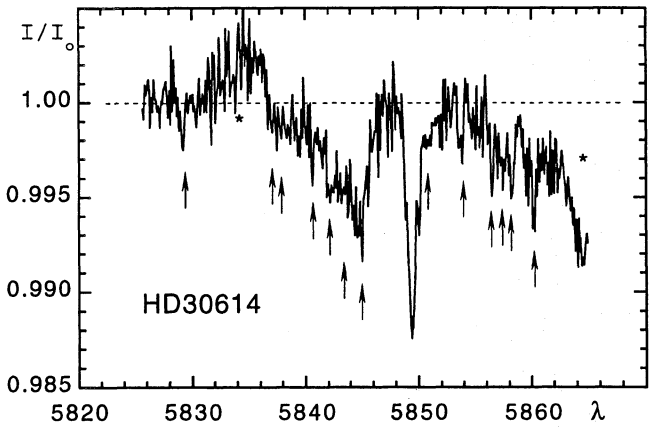

Fig. 7. High resolution spectrum of HD30614 (09.5 Ia, E_{B-V} = 0.30, Vsin(i) = 174 km/s) - OHP data.

this to be an unrelated DIB λ5850.2, but note that the width is uncharacteristic between narrow and broad DIBs (Jenniskens & Désert 1995).

The features on the red and blue side of λ5850 are of special interest, because they may be part of the intrinsic profile of λ5850. They are not of instrumental or photospheric origin given

Table 2. Summary of Diffuse Interstellar Bands in the wavelength range between 5830 and 5862 Å. The position of each DIB, the Full Width at Half Maximum (FWHM) and the central depth (A_c) refer to the spectrum of HD167264 (E_{B-V} = 0.28). Also given are equivalent width (W) per unit reddening for the line of sight to HD183143 (E_{B-V} = 1.24). While wavelength positions should be accurate to ±0.1 Å, systematic errors can be as large as ±0.3 Å. The FWHM includes the instrumental resolution of 0.098 Å and the broadening due to Doppler motion in the cloud which is believed to be less than 0.2 Å. Cross references: λ5844 and λ5850 were mentioned by Herbig (1975), other references are Krelowski et al. (1993) and Jenniskens & Désert (1994). Symbols "+", "o", and "-" mark the DIB identification of an absorption feature as "certain", "probable", and "possible" respectively, following Jenniskens & Désert (1994).

	λ_c	FWHM Å	Ac	W/E_{B-V} HD167264	W/E_{B-V} HD183143	cross ref.
+	5837.9	0.52	0.0030	6	1	-
-	5838.5	0.50	0.0017	3	-	-
+	5840.7	0.50	0.0043	8	4	-
+	5842.1	0.24	0.0063	6	6	-
o	5842.7	0.80	0.0025	5	2	-
+	5843.4	0.80	0.0025	5	5	-
+	5844.5	4.0	0.0040	50	58	λ5844
+	5844.8	0.47	0.0067	12	11	K93
o	5845.4	0.70	0.0025	7	5	-
-	5846.0	1.3:	0.0012	6	6	-
o	5847.7	0.61	0.0025	6	3	-
+	5849.7	0.53	0.0376	76	43	λ5850
+	5850.2	1.5	0.0056	32	8:	-
-	5852.0	5.:	-	-	23:	JD94
o	5853.2	0.26	0.0029	3	-	-
o	5855.5	0.31	0.0024	3	-	-
o	5856.5	0.26	0.0056	6	-	-
o	5857.2	0.28	0.0044	5	-	-
-	5860.2	0.23	0.0044	4	-	-

the similarity of the spectrum of our B0Ia star HD167464 (ESO) and the spectrum of the B2V star HD147889 of Krelowski et al. (CFHT). Also, the instrumental resolution varies from 0.14 in the first two spectra of Fig. 8 to 0.098 in the latter three and is small compared to the width of the DIB, which is about 0.48 Å wide. The shape and width of each profile may be affected by the turbulent motion in the ISM and different cloud components in the line of sight. However, these variations do not cause the observed features. For example, the KI profile of HD30614 at 0.3 Å resolution is given in Jenniskens & Désert (1994) and consists of a narrow main peak of FWHM = 0.34 Å (including instrumental broadening) and a faint component of intensity ratio 1 : 0.18 displaced by -0.35 Å to the blue. Hence, this cloudlet can not account for the feature on the red side of the DIB profile. For HD167264, McRae and Spitzer (1952) give two additional components in the interstellar NaI-D2 line with intensity ratios 1 : 0.11 : 0.15 at -0.29 Å and -0.74 Å respectively, which also can not account for the DIB profile shape. The NaI-D profiles of other lines of sight are not available, but the sharpness

of the weak DIBs superposed on λ5844 in these lines of sight (e.g. Fig. 5) imply that there is a small radial velocity dispersion in cloud motion. Hence our conclusion that the Doppler shifted cloud components and turbulent motion are not responsible for the features on the blue and red side of λ5850.

3.6. Relative band strength variations

There are significant variations of relative band strength between λ5844 and λ5850 as well as among the weak DIBs in this spectral range. Compare the band strength of these DIBs in HD167264 and HD183143 (Table 2), derived from a reconstruction of the complex profile by a sum of Gaussians. These represent lines of sight with relatively weak and strong λ5844. A comparison of numbers shows that some of the weaker DIBs do seem to correlate with λ5844 better than with λ5850, such as λ5844.8, and perhaps λ5843.4 and λ5840.7, while others are relatively weak in HD183143, notably λ5840.7 and λ5837.9, which seem to follow λ5850. Such band strength variations are also found in other profiles, where the four features are usually strong when λ5844 is weak but only λ5844.8 is clearly present when λ5844 is strong.

It is possible that some of these bands form a single complex DIB. The λ5844 profile in combination with λ5844.8 and some of the weak features bear resemblance to the complex λ5778/λ5750 (Fig. 1). Both structures have two possibly related features on the blue side of the main band (λ5843.4 and λ5842.1) and a steep shoulder on the red side. There is, however, no further evidence for this conjecture.

3.6.1. Correlation with gas kinetic temperature

In search of band strength and band shape variations with kinetic temperature, the strength of the strongest DIBs (Table 3) are compared to the rotational temperature of molecular hydrogen (T_{01}) in the line of sight as given by the population distribution in the J = 0 and J = 1 states derived from Copernicus observations (Savage et al. 1977). This rotational temperature is proportional to the kinetic temperature of the molecular gas and indicative of the kinetic temperature of the gas in which the DIBs are found. Although the diffuse interstellar bands are linked to the atomic HI gas more than to the molecular H_2 gas (Herbig 1993, Jenniskens et al. 1994), the observed lines of sight have about similar total column densities ($E_{B-V} \sim 0.3$) and the ratio of molecular to atomic gas does not vary much.

It is found that the normalised strength λ5844/E_{B-V} correlates with T_{01}, but the normalised strength of λ5850 does not. A least-squares-fit results in correlation coefficients of r = 0.78 and 0.04 respectively, before correction for measurement uncertainty. The ratio of band intensities of λ5844/λ5850 (Fig. 9) varies as a function of T_{01} temperature (r = 0.81). It is known that T_{01} is low for clouds with high hydrogen density (Savage et al. 1977) and, therefore, it is not surprising that there is also a positive albeit less perfect correlation with the parameter n= $N(HI+H_2)/d$ (d is the distance to the program star), which is roughly the average hydrogen volume density (in atoms/cm^3). A linear fit in a plot of DIB strength ratio versus n^{-1} has r =

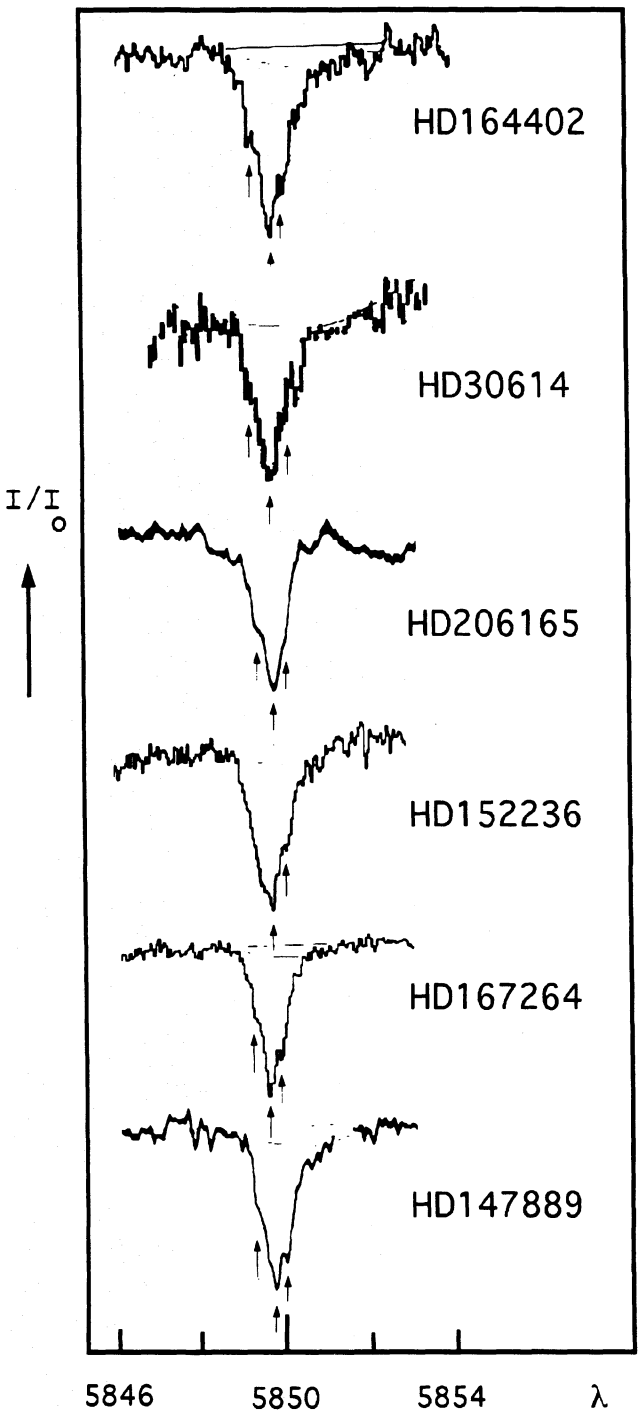

Fig. 8. Profile of λ5850 in those spectra of high signal-to-noise that have relatively narrow NaD profiles. The spectra are ordered from top to bottom in a sequence of decreasing rotational temperature of H_2 (J=0,J=1) T_{01} (Savage et al. 1977) or decreasing slope of the linear c_2 and non-linear c_4 rise of the UV extinction curve (Jenniskens & Greenberg 1993). Notes: HD164402 (B0Iab - 106K), HD30614 (09.5Ia - 80K, c_2=0.91; c_4 = 0.14), HD206165 (B2Ib - c_2 = 0.94; c_4 = 0.56; from Krelowski et al. 1993), HD152236 (B1Iae - c_2 = 0.85; c_4 = 0.38), HD167264 (B0Ia - 77K), and HD147889 (B2V - <50K, c_2 = 0.11; c_4 = 0.88; from Krelowski et al. 1993).

Table 3. DIB absorption intensity at 5844.1 Å and 5849.7 Å for lines of sight in which the rotational temperature of H_2 and the gas density have been measured. K = Krelowski (1989), Krelowski et al. (1993), and Krelowski & Sneden (1993), H = Herbig (1993), and J = this work. The rotational temperature of H_2 (T_{01}), n(HI+H_2), and the logarithm of H_2 and HI column densities are from Savage et al. (1977). E_{B-V} values are from Savage et al. and are compared to values derived from photometric data in the Hipparchos Input Catalogue using the Fowler 1977 scale (E^h_{B-V}).

Star	E_{B-V}	E^h_{B-V}	T_{01} K	n H+2H$_2$ cm^{-3}	log N H_2 cm^{-2}	log N HI cm^{-2}	Ac 5844	Ac 5850	
HD23180	0.30	0.23	48	2.2	20.6	20.9	.003	.047	K
HD149757	0.32	0.35	54	3.3	20.7	20.7	.001	.020	H
HD24398	0.33	0.44	57	1.3	20.7	20.8	.002	.026	H
HD22951	0.24	0.28	63	1.3	21.0	21.2	.003	.021	H
HD199579	0.36	0.38	74	0.50	20.1	20.0	.002	.009	K
HD167264	0.28	0.30	77	0.37	20.0	20.0	.004	.051	J
HD30614	0.32	0.32	80	0.35	20.3	20.9	.004	.016	J
HD2905	0.35	0.30	104	0.64	20.3	21.2	.007	.024	K
HD164402	0.20	0.22	106	0.25	19.0	19.3	.005	.026	J
HD183143	-	1.24	-	-	-	-	.024	.072	J

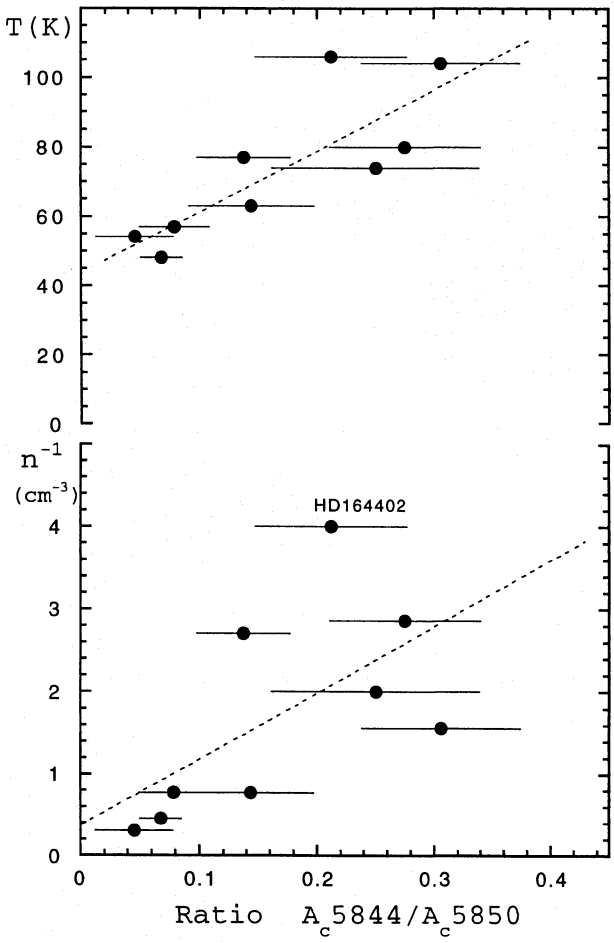

Fig. 9. Ratio of band intensity of DIBs 5844/5850 versus the rotational temperature in the J = 0 and J = 1 levels of molecular hydrogen and the line of sight mean density: n = N(H)/d. The 5844 DIB is less deep in cool lines of sight.

0.62 (Fig. 9). Of course, n^{-1} is less well determined than T_{01}, which lowers the correlation coefficient.

The varying relative strength of λ5844 does not lead to changes in band shape or position. The pattern of weak features superposed on λ5844 changes with increasing relative strength of λ5844 versus λ5850 and, hence, with T_{01}.

There is no clear indication that the shape of the λ5850 profile, its width and the presence of the red and blue shoulders, changes with increasing T_{01}. The profiles of HD164402 and HD30614, however, show a more pronounced red grading than those of the colder HD167264 and HD147889 lines of sight (Fig. 8).

4. Discussion

The previous results argue against the hypothesis that λ5844 and λ5850 are the R and Q branch of a rovib profile. Although the band shape changes as a function of kinetic temperature, the center of the band and the width do not vary significantly. The relative band intensity of the weak DIBs superposed on λ5844 change but, in the process, the features that must be the highest rotational levels do not become relatively more intense with increasing temperature. λ5844's intensity goes to zero for low kinetic temperature (< 40 K), which is also inconsistent. We do not see strong changes in the Q-branch (the λ5850 profile) when the band ratio of λ5844 versus λ5850 changes. The expected P-branch at 5852 Å is not detected with certainty, although some spectra suggest the presence of a weak broad band with only a fraction of the intensity of λ5844. Of course, the band ratios are also not understood if the rotational population in the ground state is maintained by a selective excitation and de-excitation mechanism, which potentially could keep the rotational population independent of kinetic temperature.

An alternative interpretation for the observed band shape variations, and in our opinion the more likely, is that most absorption features are unrelated and that the variations merely reflect the behaviour of different DIB families in different type of environments (Chlewicki et al. 1986, Krelowski & Walker 1987, Benvenuti & Porceddu 1989, Porceddu et al. 1991). The ratio of intensities of DIBs λ5844 and λ5850 could reflect, for example, the balance between ionization and recombination, which can be different for different molecules (Jenniskens et al. 1994, Ehrenfreund et al. 1995). Alternatively, the band intensity can perhaps be affected by chemical alteration of the molecules. Krelowski et al. (1993) found that the relative strength of λ5844 correlates with the shape of the extinction curve. Extinction curve variations are also a function of local environment, where the dense medium with low values of T_{01} is the site of accretion of small grains on the larger grains resulting in a less steep linear rise in the extinction curve (e.g. Jenniskens & Greenberg 1993).

The lack of resolved rovib profiles with a central Q-branch in the DIB Survey makes it unlikely that many of the close pairs of DIBs present in the survey are other than chance superpositions.

That does not exclude that some DIBs may show resolved rovib structure at higher spectral resolution. Indeed, the features on the red and blue side of λ5850 could well be the R, Q and P branch of an unresolved DIB, in the light of similar, but more pronounced, features seen in the profile of λ6613 (Hibbins et al. 1995). The separation between the maxima of the possible P and R branches, as indicated by the arrows in Fig. 8, is about 0.69 Å or 2.0 cm^{-1}. This value is in between the separation of 0.62 Å or 1.4 cm^{-1} found for λ6613 and 0.77 Å or 2.3 cm^{-1} for λ5797 (Hibbins et al. 1995, Sarre et al. 1995). The red feature stands out more clearly from the central peak and has a red grading, while the sharp short wavelength edge of the blue shoulder could signify a band inversion. Such a progression of rotational lines is the result of a small decrease of the rotational constant in the excited state. Both λ5850 and λ5797 show this effect but the band shapes are slightly different, which argues against both bands being part of a vibrational progression.

This interpretation of the shape of the λ5850 absorption band is consistent with the position and shape of the Red Rectangle emission band that has been associated with λ5850 (Sarre 1991, Fossey 1991). The emission band is found longward of λ5850 and progressively moves further away from 5850 Å with decreasing distance to the exciting central star (Miles et al. 1995, Sarre et al. 1995a).

The presence of rotational structure in the electronic transitions of the narrower DIBs puts other observations in place. It is an elegant explanation of the find that absorptions with widths as narrow as the interstellar lines are few in the DIB spectrum (Jenniskens & Désert 1995). Hence, it is likely that rotational broadening makes the narrow Diffuse Interstellar Bands "diffuse", whereas internal conversion or some other form of lifetime broadening can be responsible for other DIBs being broad or very broad (Leach 1993).

5. Conclusions

We discard the possibility that λ5844 and λ5850 form the R and Q branch of a single rovib profile, but find instead that the λ5850 has substructure that is reminiscent of an unresolved rovib profile, with a narrow central peak and two shoulders, one on the blue and one on the red side.

Four weak features are superposed on the broad λ5844. Although they are most likely unrelated absorptions, we do notice the conspicuous similarity with features superposed on the broad λ5778. There are significant variations of relative intensity of these features from one line of sight to another, that correlate with relative intensity of λ5844 and λ5850.

The relative intensity of λ5844 and λ5850 correlates with the line of sight rotational temperature in the J=0 and J=1 levels of molecular hydrogen T_{01}. Although this empirical relationship may merely reflect environmental changes, it can be applied to indirectly measure the kinetic temperature of the molecular gas by visual absorption spectroscopy.

Now that structure reminiscent of a rovib profile has been detected in the relatively weak DIB λ5850, it is not unlikely that future studies will find such structure in many more DIBs, which can prove an important tool in identifying the DIB carriers.

Acknowledgements. We thank the observing staff at OHP and ESO for their generous support during the observations. PJ acknowledges the Stazione Astronomica in Cagliari for an invitation that enabled a visit in October of 1994. This paper also benefitted from discussions with Janet Miles, Rob Hibbins and Peter Sarre at Nottingham University. We thank David F. Blake for his support of the project at NASA/Ames Research Center.

References

Benvenuti P., Porceddu I., 1989, A& A 223, 329.
Bernacca P.L., Perinotto M., 1970, Contributi Osservatorio Astrofisico di Padova in Asiago, 239, 1.
Chlewicki G., van der Zwet G.P., van IJzendoorn L.J., Greenberg J.M., Alvarez P.P., 1986, ApJ 305, 455.
Cossart-Magos C., Leach S., 1990, A& A 233,559.
Danks A.C., Lambert D.L., 1976, MNRAS 174, 571.
Désert F.-X., Jenniskens P., Dennefeld M., 1995, A& A 303, 223.
Douglas A.E., 1977, Nature 269, 130.
Ehrenfreund P., Foing B.H., d'Hendecourt L., Jenniskens P., Désert F.-X., 1995, A& A 299, 213.
Fossey S.J., 1991, Nature 353, 393.
Gillet D., 1990, OHP Aurelie User's Manual.
Hayden-Smith Wm., Snow T.P., Jura M., Cochran W.D., 1981, ApJ 248, 128.
Herbig G.H., 1975, ApJ 196, 129.
Herbig G.H., Soderblom D.R. 1982, ApJ 252, 610.
Herbig G.H., 1993, ApJ 407, 142.
Hibbins R.E., Miles J.R., Sarre P.J., Fossey S.J., Somerville W.B, 1995, in The Diffuse Interstellar Bands. A.G.G.M. Tielens, T.P. Snow (eds.), p. 25.
Jenniskens P., Greenberg J.-M., 1993, A& A 274, 439.
Jenniskens P., Désert F.-X., 1993, A& A 274, 465.
Jenniskens P., Désert F.-X., 1994, A& AS 106, 39.
Jenniskens P., Ehrenfreund P., Foing B., 1994, A& A 281, 517.
Jenniskens P., Désert F.-X., 1995, in The Diffuse Interstellar Bands, A.G.G.M. Tielens, T.P. Snow (eds.), p. 39.
Josafattson K., Snow T.P. 1987, ApJ 319, 436.
Krelowski J., Walker G.A.H., 1987, ApJ 312, 680.
Krelowski J., 1989, in Interstellar Dust, IAU Symp. 135, 67.
Krelowski J., Sneden C., 1993, PASP 105, 1141.
Krelowski J., Snow T.P., Papaj J., Seab C.G., Wszolek B., 1993, ApJ 419, 692.
Leach S., 1993, Observatory 114, 97.
McRae P., Spitzer L., 1952, ApJ 115, 227.
Miles J.R., Sarre P.J., Scarrott S.M., 1995, in The Diffuse Interstellar Bands, A.G.G.M. Tielens, T.P. Snow (eds.), p. 143.
Moore C.E., 1945, Contr. Princeton Univ. Obs., No. 20.
Porceddu I., Benvenuti P., Krelowski J., 1991, A& A 248, 188.
Sarre P.J., 1991, Nature 351, 356.
Sarre P.J., Miles J.R., Kerr T.H., Hibbins R.E., Fossey S.J., Somerville W.B., 1995, MNRAS 277, L41.
Sarre P.J., Miles J.R., Scarrott S.M., 1995a, Science 269, 674.
Savage B.D., Bohlin R.C., Drake J.F., Budich W., 1977, ApJ 216, 291.
Snell R.L., Vanden Bout P.A., 1981, ApJ 244, 844.
Welter G.L., Savage B.D., 1977, ApJ 215, 788.